minerals

Article

Reservoir Characterization of Alluvial Glutenite in the Guantao Formation, Bohai Bay Basin, East China

Qing Li [1,2], Xuelian You [3,*], Yuan Zhou [1,2], Yu He [4], Renzhi Tang [5] and Jiangshan Li [1,2]

1. National Key Laboratory of Petroleum Resources and Engineering, Beijing 102249, China; liqing@cup.edu.cn (Q.L.)
2. College of Geosciences, China University of Petroleum (Beijing), Beijing 102249, China
3. School of Ocean Sciences, China University of Geosciences (Beijing), Beijing 100083, China
4. Research Institute of Petroleum Exploration and Development, Beijing 10083, China
5. Zigong Earthquake Monitoring Center, Seismological Bureau of Sichuan Province, Zigong 643000, China

* Correspondence: youxuelian@cugb.edu.cn

Abstract: Alluvial glutenite reservoirs have obviously stronger heterogeneous and more complex control factors than sandstone reservoirs. Taking the Binxian Uplift area in the Boahi Bay Basin as an example, the aim of this study is to clarify the characteristics and control factors of the alluvial glutenite reservoir quality and the influence of reservoir properties on hydrocarbon accumulation. Pore types in the study area mainly include residual intergranular pores, intergranular dissolved pores, intragranular dissolved pores, and mold pores. The residual intergranular pores and intergranular dissolved pores are the main pore types. Most samples have porosity greater than 15% and permeability is mainly concentrated between 50 mD and 500 mD. It is shown that lithology type, microfacies, and diagenesis have significant impact on the reservoir quality. The reservoir qualities of very fine sandstone and fine sandstone are better than those of conglomerate and gravel-bearing sandstone. Instead of grain size, sorting affects the alluvial glutenite reservoir quality significantly. Oil-bearing samples commonly have sorting coefficient less than 2 while non-oil-bearing samples have sorting coefficient larger than 2. There are significant differences in reservoir physical properties of different sedimentary microfacies. The stream flow in mid-alluvial fan (SFMA) and braided channels outside alluvial fans (BCOA) have relatively weaker compaction and better reservoir quality than the overflow sand body (OFSB) and debris-flow in proximal alluvial fan (DFPA). Calcite cementation, the main cement in the study area, commonly developed at the base of SFMA and BCOA and near the sandstone-mudrock contacts. The source of calcium carbonate for calcite cement mainly came from around mudstone. High calcite cement content commonly results in low porosity and permeability. Individual glutenite thickness is also an important influencing factor on reservoir quality. Reservoirs with large thickness (>4 m) have high porosity and permeability. Dissolution occurred in the reservoir, forming secondary dissolution pores and improving reservoir quality. The dissolution fluid for formation of secondary pores is mainly meteoric waters instead of organic acid. The reservoir property has an important influence on hydrocarbon accumulation. The lower limit of physical properties of an effective reservoir is a porosity of 27% and permeability of 225 mD. The findings of this study can be utilized to predict the reservoir quality of alluvial glutenite reservoirs effectively in the Bohai Bay Basin and other similar basins.

Keywords: alluvial fan; glutenite reservoir; conglomerate; reservoir quality; diagenesis; porosity and permeability; drill core samples; Binxian Uplift area

check for updates

Citation: Li, Q.; You, X.; Zhou, Y.; He, Y.; Tang, R.; Li, J. Reservoir Characterization of Alluvial Glutenite in the Guantao Formation, Bohai Bay Basin, East China. *Minerals* **2024**, *14*, 317. https://doi.org/10.3390/min14030317

Academic Editors: Tivadar M. Tóth and Yubin Bai

Received: 3 February 2024
Revised: 9 March 2024
Accepted: 15 March 2024
Published: 16 March 2024

1. Introduction

Alluvial fan, which is a fan-shaped sedimentary body formed at the mouth of a mountain where streams flows out with characteristics of rapid sedimentation near the source, is commonly composed of gravel, sand, and mud, forming an alluvial glutenite reservoir with strong heterogeneity [1]. Alluvial glutenite reservoirs are important targets for petroleum exploration, such as the Garfield alluvial fan conglomerates in Kansas, USA [2], the alluvial fan in the Edvard Grieg field, Norwegian North Sea [3], and alluvial fan reservoir in the Junggar Basin, Xinjiang oilfield [4,5].

Alluvial glutenite reservoirs commonly are strongly heterogeneous because of complex and variable sedimentation and diagenetic processes [6–9]. There is various lithofacies in alluvial glutenite reservoirs and lithofacies change rapidly horizontally and vertically [10,11]. Sedimentary microfacies and diagenesis processes in alluvial glutenite reservoirs also vary greatly [3,12,13]. The various lithofacies, sedimentary microfacies, and diagenesis processes have significant impact on the quality of alluvial glutenite reservoirs [4,10,13,14]. Clarifying reservoir characteristics and assessing the role of depositional factors and diagenetic processes is critical to evaluate reservoir quality [15–18].

Numerous previous studies have focused on characteristics and control factors of sandstone reservoirs [19–21]. Compared with sandstone reservoirs, the pore structure of alluvial glutenite reservoirs is more complicated with broad pore-throat sizes ranging from 0.01 to 1000 μm and multiple pore-throat size distributions that are unimodal, bimodal or multimodal [3,22,23]. Alluvial glutenite reservoirs have obviously stronger heterogeneous and more complex control factors than sandstone reservoirs [4,5]. However, the difference in petroleum enrichment between different drilling wells in alluvial glutenite reservoirs and controlling factors on the reservoir quality and petroleum accumulation are not yet adequately clear.

The alluvial glutenite reservoirs that have developed at the Binxian Uplift area, provide a great opportunity to study the characterization and key influence factors of alluvial glutenite reservoirs. The purpose of this study is to clarify the characteristics of petrology, storage space, and pore structures in the alluvial glutenite reservoir; to figure out factors that control the alluvial glutenite reservoir quality; and to determine how lithology, sedimentary microfacies, and diagenesis affected the reservoir quality and the influence of reservoir properties on hydrocarbon accumulation. The findings of this study can be utilized to predict reservoir quality effectively.

2. Geological Setting

The Binxian Uplift area is located in the northern part of Binzhou City, Shandong Province. The tectonic location of the Binxian Uplift area is in the southwest of the Jiyang Depression and Bohai Bay Basin (Figure 1a). To the north of the Binxian Uplift is the Chenjiazhuang Uplift, and to the southeast is the Lijin Sag. The north–south direction of the Binxian Uplift is limited by the Binbei Fault Zone and Binnan Fault Zone, respectively. The exploration area of the Binxian Uplift area is about 240 km^2, and the main exploration wells are distributed in the lower right part of the protrusion (Figure 1b).

The basement rock of the study area is Archean rock. The bedrocks are directly overstepped by the Paleogene Shahejie Formation (Es), Neogene Guantao Formation (Ng), and Minghuazhen Formation (Nm) (Figure 1c). This study focuses on the Guantao Formation. According to the lithology and well log characteristics, the Guantao Formation can be divided into four sand groups: Ng1, Ng2, Ng3, and Ng4 (from top to bottom), with Ng4 being the main oil-bearing interval. The Ng4 can be further divided into three layers from bottom to top: $Ng4_3$, $Ng4_2$, $Ng4_1$.

In the early sedimentary period of the Guantao Formation, the ancient uplift of Binxian was raised up and exposed at the surface, exhibiting a geomorphic feature of alternating gullies and beams, with a number of normal faults [24]. Normal faults together with later tectonic processes controlled the distribution characteristics of the Guantao Formation in the study area [25–28]. The Binnan Fault and Binbei Fault are the main co-sedimentary faults in the study area, which have an important impact on the sedimentary filling in the area [29]. The Binbei Fault basically does not develop associated secondary faults, while the southern part of the Binnan Fault developed many secondary fault structural zones, most of which are normal faults with a nearly east–west direction. The secondary fault structural zones cut the Guantao Formation into a stepped shape, providing a pathway for later oil and gas migration [30]. In addition to the differential effects of fault activity, the rate of stratigraphic subsidence, changes in accommodation space, and the amount and direction of sediment injection also affect the development of sequence patterns.

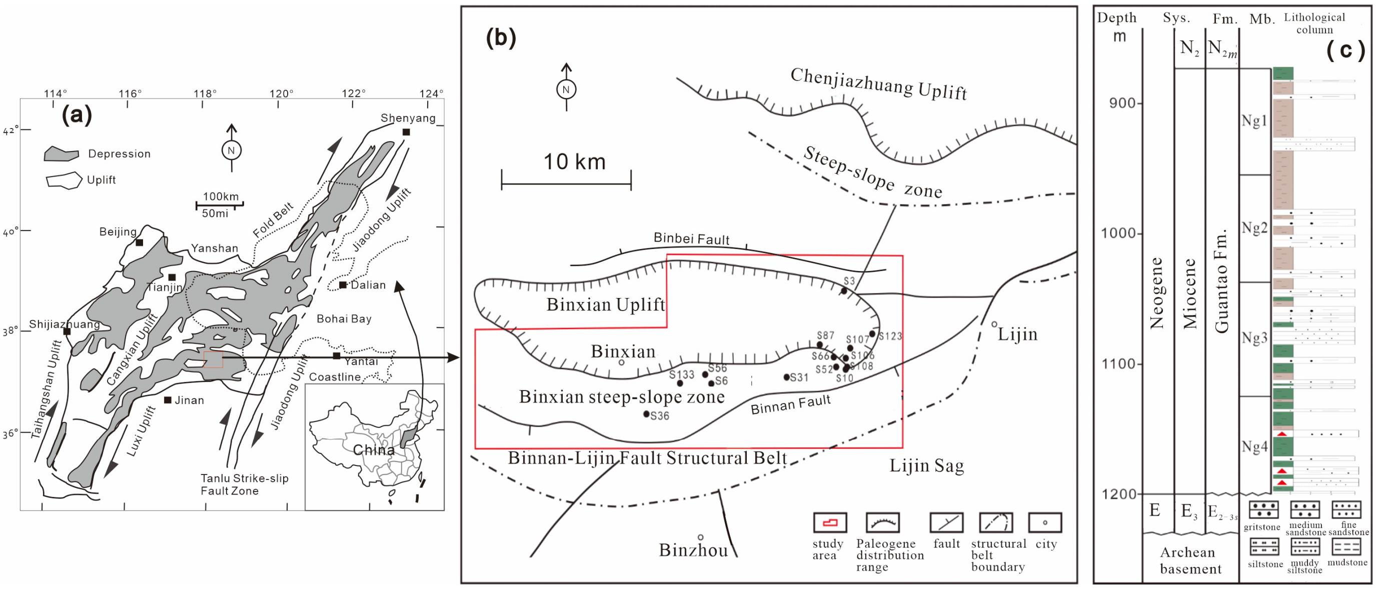

Figure 1. The geographical location of Binxian area and the stratigraphic division of the target interval. (**a**) Tectonic map of Bohai Bay Basin; (**b**) Structural map of Binxian uplift and its periphery; (**c**) Stratigraphic development characteristics of the study area.

The Guantao Formation in the study area is a set of alluvial fan—fluvial sedimentary systems. In the early stage of the Guantao Formation, alluvial fans developed near the Binxian uplift and braided river sediments developed in the surrounding areas. In the middle and later stages of the Guantao Formation, the Binxian uplift was gradually covered, and the braided river transitioned into a meandering river.

3. Samples and Methods

A total of 45 samples were obtained from well-cores of alluvial glutenite reservoirs of the Guantao Formation in the study area (Figure 1). The samples were mainly collected from six exploration wells (S56, S63, S87, S106, S108, and S17). Samples were collected for thin section preparation. Among them, 30 samples were collected for grain size, porosity, and permeability analysis. Ten samples were chosen for X-ray diffraction analysis (XRD), scanning electron microscope analysis (SEM), and mercury injection experiments.

In order to highlight and observe pores, samples collected for thin section were impregnated with red resin before thin sectioning. X-ray diffraction (XRD) was used to analyse mineralogical characteristics and content. Samples were oven-dried and ground to powder prior to XRD analysis. XRD analyses was performed by a D8 Discover instrument with Cu–Ka radiation. The voltage and current parameters were 40 kV and 25 mA, respectively. Semiquantitative analysis of the relative abundance of various mineral phases was performed by the analysis of diffractograms.

Plugs with diameter of 2.5 cm were drilled from cores for porosity and permeability analysis. The porosities were measured according to Boyle's law and Darcy's law of gas percolation by a helium porosimeter. The porosity and permeability were measured by meter CAT112 and CAT113 from American CoreLab in the United States. The scanning electron microscopy (SEM) was used to study pore structure, pore types, pore size and distribution, and mineral characteristics. The SEM was performed by the Quanta 200 F produced by FEI Corporation (Hillsboro, OR, USA). Mercury injection experiments were used to study pore structure by using the American core-lab CMS300 and AutoPore IV 9505 mercury intrusion instruments from United States.

4. Results

4.1. Petrology Characteristics

4.1.1. Lithological Characteristics

According to the observation and analysis of well cores, the rock of the Guantao Formation in the study area mainly included the following lithology types: conglomerate (Cg), gravel bearing coarse sandstone (GS), medium sandstone (MS), fine sandstone (FS), very fine sandstone (VFS), siltstone (ST), and mudstone (MD) (Figure 2). Various rock types indicated the variability of the sedimentary environments. In the study area, mudstone has the highest proportion, mainly consisting of purplish red and variegated colors (Figure 2F).

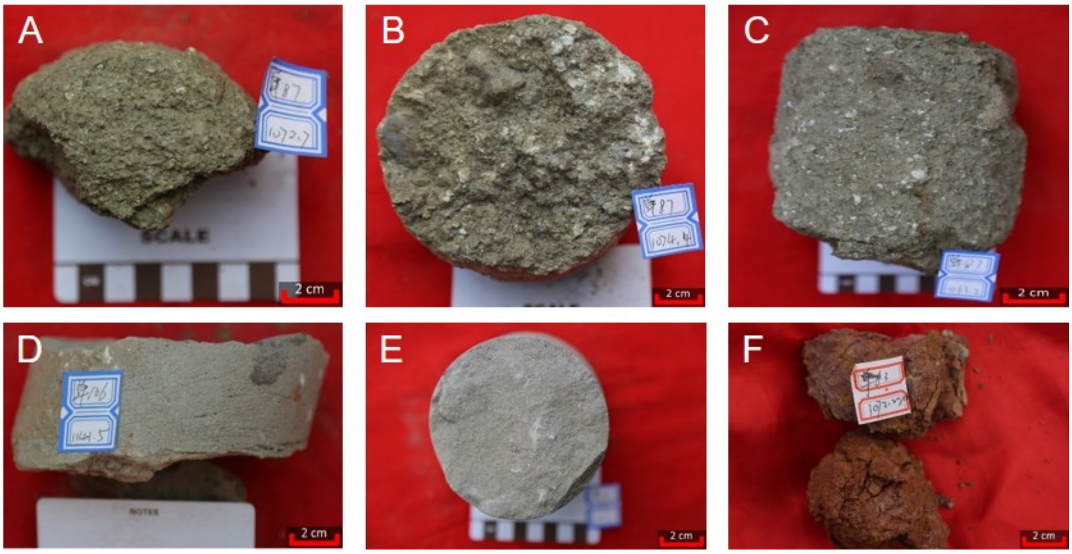

Figure 2. Lithologic types in the study area. (**A**) Massive grayish green gravel-bearing coarse sandstone, matrix supported, poorly sorted, well S87, 1072.7 m, Ng4; (**B**) Massive conglomerate with poor roundness and sorting, well S87, 1074.4 m, Ng4; (**C**) Massive muddy conglomerate, poor sorting and rounding, well S87, 1071.7 m, Ng4; (**D**) Medium-fine sandstone with cross bedding, S106, 1141.5 m, Ng4; (**E**) Very fine sandstone, S56, 1117 m, Ng4; (**F**) Purple red mudstone, S63, 1072.23 m, Ng4.

Conglomerates and gravel bearing sandstones are mainly developed in the Ng4 sand group near the Binxian uplift. Gravels in the conglomerates are mainly granite, occasionally sandy with poor roundness and sorting (Figure 2A–C). The diameters of gravels are up to 9 cm. Sandstone is mainly fine sandstone and very fine sandstone (Figure 2D,E), which are the main reservoir rocks in the study area. The interstitial materials in the conglomerates are mainly carbonate and mudstone. According to point counting of thin sections, the detrital components of sandstone in the study area comprise quartz (main 40%–73%), feldspar (9%–50%), and rock fragments (10%–60%). Based on Folk (1980) [31], the sandstones are mainly lithic arkose and feldspathic litharenite (Figure 3). There are obvious differences in the composition of different layers. From $Ng4_3$ to Ng3 layer, sandstone change from litharenite, to feldspathic litharenite, and then to lithic arkose and arkosic arenite. Unstable rock debris content keeps decreasing while the feldspar content keeps increasing from the $Ng4_3$ to the Ng3 layer. The proportion of mudstone in the Guantao Formation gradually increases from bottom to top.

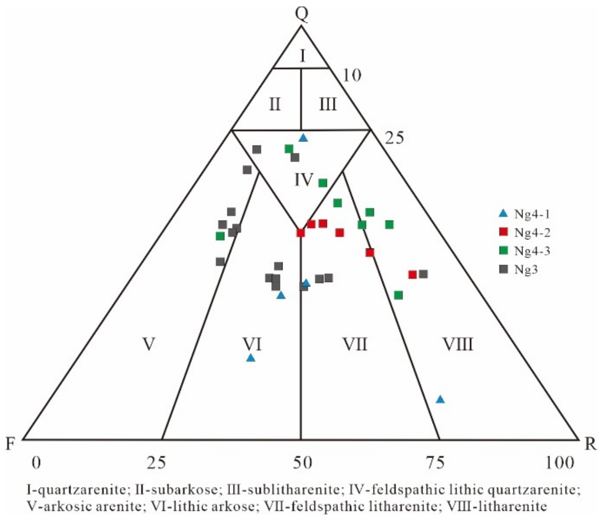

Figure 3. QFR detrital composition of the Guantao formation samples in this study, based on the classification of Folk (1980) [31]. I-quartzarenite; II-subarkose; III-sublitharenite; IV-feldspathic lithic quartzarenite; V-arkosic arenite; VI-lithic arkose; VII-feldspathic litharenite; VIII-litharenite.

4.1.2. Textural Characteristics

Based on core observations, thin section analysis, and grain size analysis, the particle size variation range of the Ng4 group is large, ranging from fine silt to gravel size. The rocks have low composition and textural maturity. There is a significant difference in sorting and median particle size of different wells, showing strong heterogeneity (Figure 4). It can be seen that conglomerates often have mixed particles with different sizes, showing poor sorting. However, the particle size of fine sandstone and very fine sandstone is relatively uniform and presents relatively good sorting (Figure 4). The particle size in different layers also varies obviously. The median particle size decreases from $Ng4_3$ to $Ng4_1$ (Figure 5). In the Ng4 sand group, the closer to the Binxian uplift, the poorer the maturity of composition and texture.

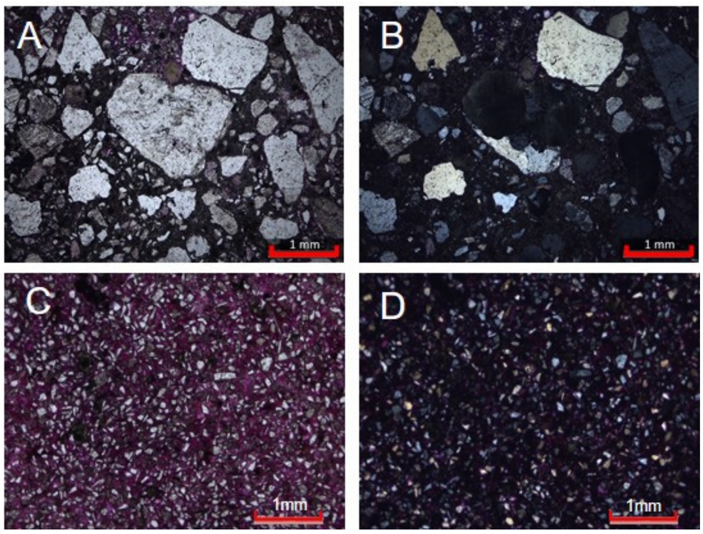

Figure 4. Microscopic characteristics of conglomerate and sandstone. (**A**) Conglomerate, showing poor sorting, under plain light, well S63, 1131.3 m, $Ng4_3$; (**B**) Conglomerate, showing poor sorting, under cross-polarizers, well S63, 1131.3 m, $Ng4_3$; (**C**) Very fine sandstone, showing well sorting, under plain light, well S63, 1126.8 m, $Ng4_3$; (**D**) Very fine sandstone, showing well sorting, under cross-polarizers, well S63, 1126.8 m, $Ng4_3$.

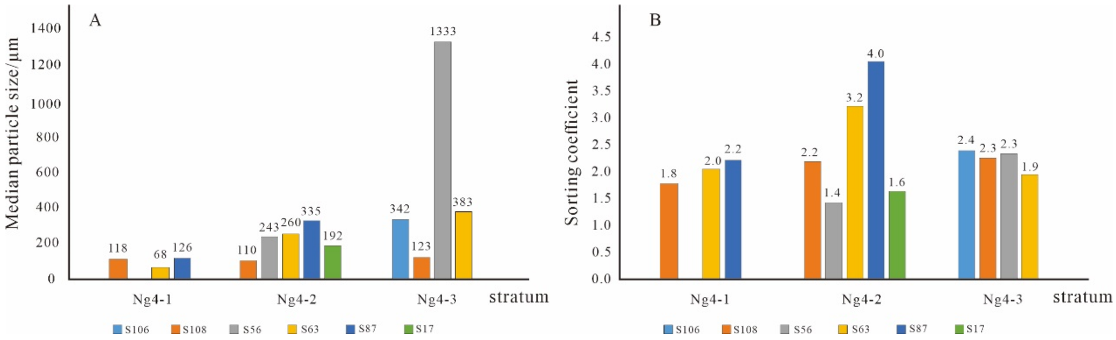

Figure 5. The median particle size and sorting coefficient of different layers from $Ng4_3$ to $Ng4_1$. (**A**) The median particle size of different layers. (**B**) The sorting coefficient of different layers.

4.2. Storage Space and Pore Structure

4.2.1. Pore Types

Pore types and pore structure are important criteria for determining the physical properties of reservoirs. Based on the thin section and SEM image analysis, the characteristics and appearance of the reservoirs have been studied. Pore types in the study area mainly include residual intergranular pores, intergranular dissolved pores, intragranular dissolved pores, and mold pores, etc. (Figure 6). Residual intergranular pores are the remaining primary pores after compaction (Figure 6A–C). Intergranular dissolved pores are intergranular pores that were later affected by dissolution (Figure 6D–F). Internal dissolution of feldspar, unstable rock debris, and carbonate cement can generate intragranular pores (Figure 7A–C). When some rock debris particles are completely dissolved, mold pores are formed (Figure 7D,E). The residual intergranular pores and intergranular dissolved pores are the main pore types in the study area, while the amount of intragranular dissolved pores, and mold pores are relatively small. Micro-fractures also developed in the reservoir (Figure 7F), which can further effectively improve the permeability of reservoirs.

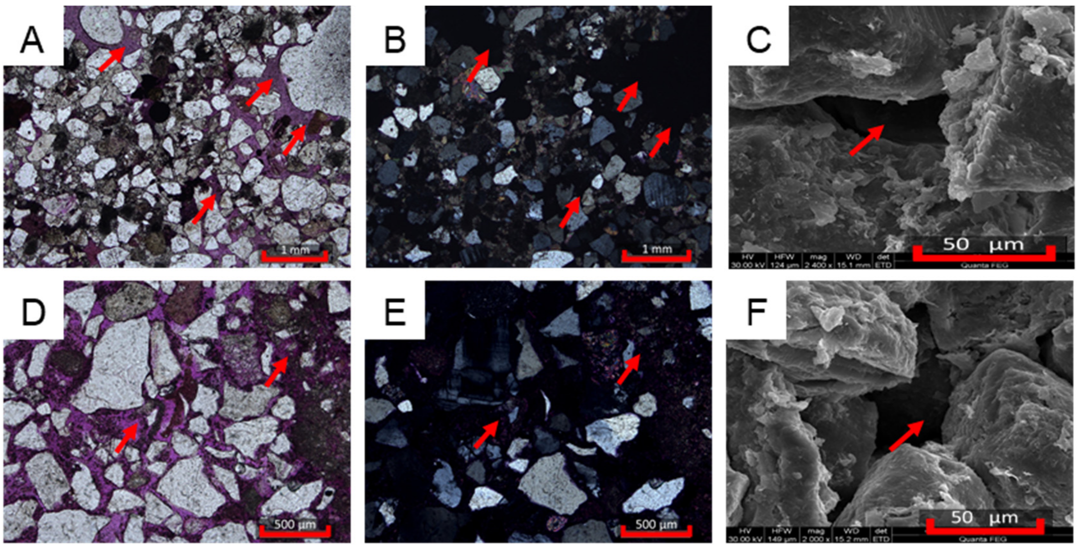

Figure 6. Characteristics of intergranular pores and intergranular dissolved pores in the alluvial glutenite reservoir. (**A**) Intergranular pores (red arrows), under plain light, well S56, 1117.9 m, $Ng4_3$; (**B**) Intergranular pores (red arrows), under cross-polarizers, well S56, 1117.9 m, $Ng4_3$; (**C**) Intergranular pores (red arrows), under SEM, well S56, 1117.9 m, $Ng4_3$; (**D**) Intergranular dissolved pores (red arrows), under plain light, well S106, 1163.4 m, $Ng4_3$; (**E**) Intergranular dissolved pores (red arrows), under cross-polarizers, well S106, 1163.4 m, $Ng4_3$; (**F**) Intergranular dissolved pores (red arrows), under SEM, well S106, 1163.4 m, $Ng4_3$.

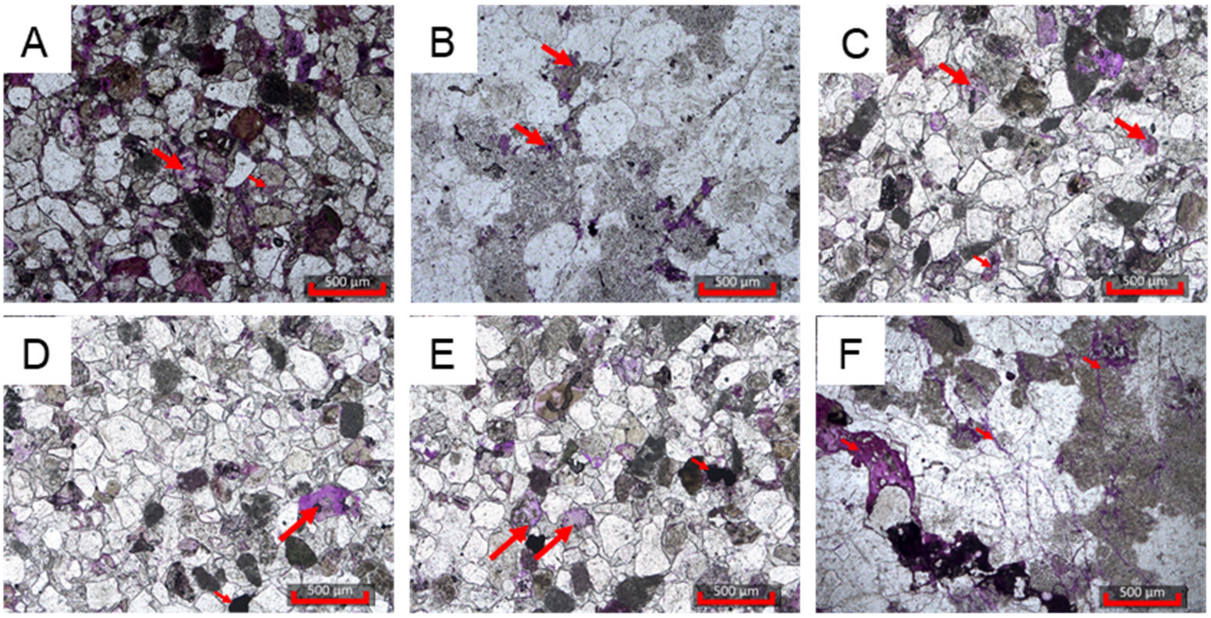

Figure 7. Characteristics of intragranular dissolved pores and mold pores in the alluvial glutenite reservoir. (**A**) Intragranular dissolved pores (red arrows), under plain light, well 56, 1095 m, $Ng4_3$; (**B**) Intragranular dissolved pores (red arrows), under plain light, well 63, 1121.2 m, $Ng4_3$; (**C**) Intragranular dissolved pores (red arrows), under plain light, well 56, 1102 m $Ng4_3$; (**D**) Mold pores (red arrows), under plain light, well 56, 1102 m, $Ng4_3$; (**E**) mold pores (red arrows), under plain light, well 56, 1102 m, $Ng4_3$; (**F**) Micro-fractures (red arrows), under plain light, well 63, 1119.2 m, $Ng4_3$.

4.2.2. Pore Structure

Pore structure refers to the type, size, distribution, and interconnectivity of pores and throats within the reservoir [5,19]. Mercury injection is one of the methods often used for testing pore structure. According to the capillary pressure curve, the pore structure in the study area can be divided into four categories (Figure 8) large pore—large throat type, medium pore—medium throat type, medium pore—fine throat type, and small pore—micro throat type. The large pore—large throat type has good, sorted pores, with capillary pressure curve tilts downwards to the left (Figure 8A). Displacement pressure of the large pore—large throat type is relatively low (0.03 Mpa) and the median radius of the pore throat is relatively large (5.376 µm). Medium pore—medium throat type has poor pore sorting, with average displacement pressure of 0.065 Ma and a median radius of the pore throat of 1.015 µm (Figure 8B). Medium pore—fine throat types have an average displacement pressure of 0.138 Mpa and an average median radius of the pore throat of 0.369 µm (Figure 8C). The small pore—micro throat type has poor pore sorting, with a relatively high displacement pressure of 0.676 Ma and a relatively small median radius of pore throat of 0.085 µm (Figure 8D). Through statistical analysis, the main pore structure in the study area is the medium pore—fine throat type.

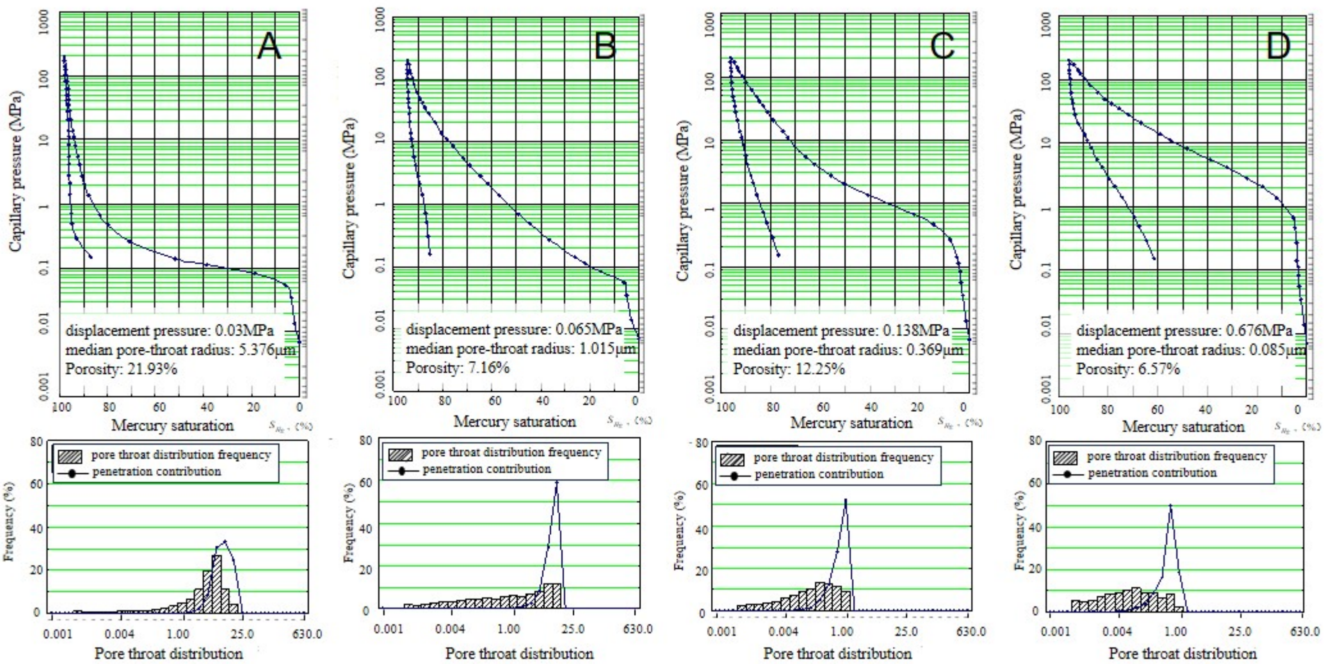

Figure 8. Different types of capillary pressure curves in the Ng4. (**A**) Large pore—large throat type, well S63, 1126.8 m; (**B**) Medium pore—medium throat type, well S63, 1131.3 m; (**C**) Medium pore—fine throat type, well S87, 1059.8 m; (**D**) Small pore—micro throat type, well S106, 1148.3 m.

4.2.3. Porosity and Permeability

The porosities and permeabilities data were obtained from the plug analysis. The reservoir has strong heterogeneity. Porosity and permeability values have a large distribution range. The porosities of samples in the study area range from 6.57% to 39.5%, with an average of 27.7% (Figure 9A). The permeabilities of the samples range from 0.14 mD to 1741 mD, with an average of 299.3 mD (Figure 9B). The average porosity and permeability of conglomerate and gravel-bearing sandstone are 15.6% and 313 mD, respectively. The average porosity and permeability of non-gravel-bearing sandstone are 31.5% and 324 mD, respectively. Most samples have a porosity greater than 15% and permeability is mainly concentrated between 50 mD and 500 mD.

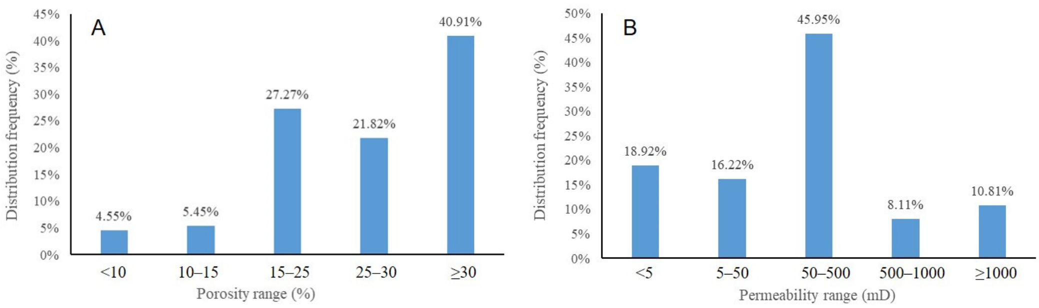

Figure 9. Porosity and permeability distribution histograms of Ng4 in the study area. (**A**) Porosity distribution histograms; (**B**) Permeability distribution histograms.

5. Discussion

5.1. Controls on Reservoir Quality

Reservoir quality is a function of multiple control factors in alluvial glutenite reservoirs, including depositional controls (such as grain sizes and sorting, etc.) and the diagenetic controls (such as cementation and compaction, etc.) [32–34]. Factors such as burial depth, temperature, and pressure might also affect diagenesis and then affect reservoir quality.

5.1.1. The Influence of Lithology on Reservoir Properties

The purplish red and variegated color mudstones indicate that the sedimentary environment was an exposed oxidation environment above water. The presence of large gravel in conglomerates indicates that the sedimentary system in the study area is near the source and had a rapid accumulation. The decrease of unstable rock debris and the increase in mudstone contents from the $Ng4_3$ to the Ng3 layer reflects a rise of the base-level. The phenomenon where the closer to the Binxian uplift the poorer the maturity of composition and texture in the Ng4 sand group indicates that sediments mainly come from the nearby Binxian Uplift, and the weathering of the Archean granite provides sources for the peripheral sedimentary system.

The lithological types of the alluvial glutenite reservoirs in the Guantao Formation in the study area mainly include conglomerates (Cg), gravel bearing coarse sandstones (GS), medium sandstones (MS), fine sandstones (FS), and very fine sandstones (VFS). A total of 43 VFS, 14 FS, 9 MS, and 23 GS have been collected for porosity and permeability analysis. The physical properties are closely related to the lithology type of the reservoir in the study area. The analysis results show that most VFS have a porosity between 30% and 40%, followed by FS, MS, Cg, and GS (Figure 10A). The porosity of VFS have the highest value among all lithologies, commonly higher than 30% (Figure 10B,C). The physical properties of very fine sandstone and fine sandstone are relatively good. On the contrast, gravel bearing sandstone and conglomerates commonly have poor reservoir qualities. The reservoir qualities of very fine sandstone and fine sandstone in the area are generally better than those of gravel-bearing sandstone and conglomerate (Figure 10).

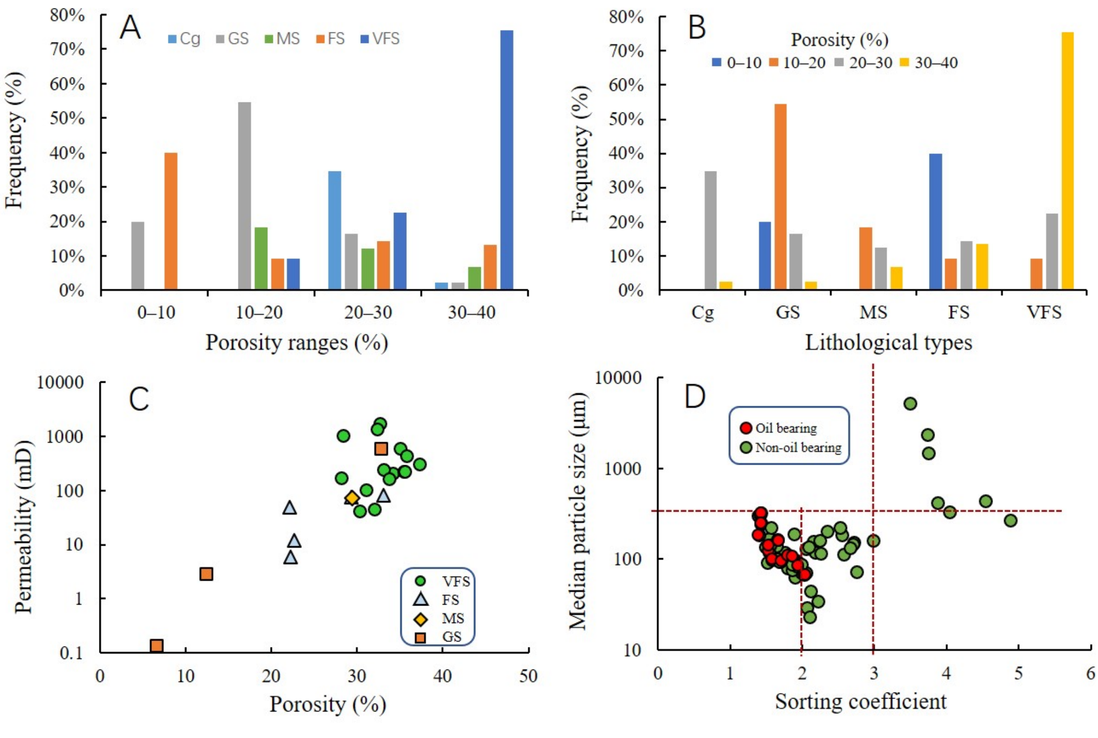

Figure 10. Differences in porosity and permeability of different lithologies. (**A**) The proportion of different lithologies in different porosity ranges; (**B**) Porosity differences in different lithological types; (**C**) Cross plot of porosity and permeability of different lithologies. (**D**) Cross plot of sorting coefficient and median particle size; Cg: conglomerate, GS: gravel-bearing sandstone, MS: medium sandstone, FS: fine sandstone, VFS: very fine sandstone.

Particle size and sorting are important factors affecting reservoir properties. According to thin section and particle size analysis, the most favorable reservoir rock types for Ng4 in the study area are very fine sandstone and fine sandstone, which have good sorting and less cementation (Figure 4). In contrast to the assumption that high porosity-permeability often corresponds to large grain sizes, the data in the study area show that lithology with large debris particles do not have high porosity and permeability but low porosity and permeability, such as conglomerates and gravel bearing coarse sandstones, suggesting that grain size is not the main factor that controls alluvial glutenite reservoir quality.

According to thin section and particle analysis, the sorting of the very fine sandstone and fine sandstone, which have high porosity and permeability, is commonly good (Figures 4 and 10D). In contrast, sorting of conglomerate and gravel bearing sandstone is poor and the porosity and permeability are also low (Figures 4 and 10D). This indicates that sorting is one of the important factors affecting alluvial glutenite reservoir quality. Samples with poor sorting have mixed particles with different grain sizes and small particle filled intergranular pores, significantly reducing porosity and permeability and damaging reservoir quality (Figure 4A,B). Matrix content also influences reservoir quality effectively. Sandstone with poor sorting commonly have high matrix content, resulting in poor filling and a reduction in porosity.

The cross plot of the sorting coefficient and median particle size shows that the median value of particle size has a certain relationship with sorting. Samples have large median particle sizes (>330 μm) and have poor sorting (with sorting coefficient >3). Because poor sorting leads to poor reservoir properties, samples with large median particle sizes, such as sorting of conglomerate and gravel bearing sandstone, have low porosity and permeability. Samples with median particle size <330 μm have a wide sorting coefficient from 1.39 to 3, among which oil-bearing samples commonly have a sorting coefficient less than 2 while non-oil-bearing samples have sorting coefficient larger than 2. This further illustrates that sorting degree is an important factor controlling reservoir quality and oil accumulation of alluvial glutenite reservoirs. In the study area, lithologies with sorting coefficient <2, mainly very fine sandstone and fine sandstone, commonly have better physical properties and oiliness.

5.1.2. Microfacies Impact on Reservoir Properties

The sedimentary microfacies in the study area mainly include: debris-flow in proximal alluvial fan (DFPA), stream flow in mid-alluvial fan (SFMA), over flow sand body (OFSB), sheet flow in distal alluvial fan (SFDA), and braided channels outside alluvial fans (BCOA) (Figure 11).

Debris-flow in proximal alluvial fan (DFPA) The proximal alluvial fan is commonly a rapidly accumulating sedimentary body at the canyon in the Binxian uplift. DFPA is a typical sedimentary microfacie in the proximal reaches of alluvial in areas of high rainfall. DFPA is commonly rich in relatively coarse sediment. The lithology in DFPA is mainly gravel-bearing sandstone or conglomerate with massive bedding.

Stream flow in mid-alluvial fan (SFMA) is formed by convergence of flow from the proximal alluvial fan to the perennial discharge stream in the mid-alluvial fan. SFMA mainly develops in the descending plate of synsedimentary faults in the Binxian uplift. The lithology in SFMA is mainly very fine to coarse sandstone with parallel bedding or intersecting bedding. A single SFMA sand body commonly has upward-fining rhythm with a thickness of approximately 5 m.

Overflow sand body (OFSB) refers to the sedimentation of sand bodies formed by the flood fluids overflowing the embankment of the channel during flood periods and is deposited outside stream channels. The OFSB is composed of medium–fine sandstone and gravel-bearing sandstone. The OFSB commonly has an upward-coarse rhythm or a complex rhythm with a thickness of between 2 m and 3 m.

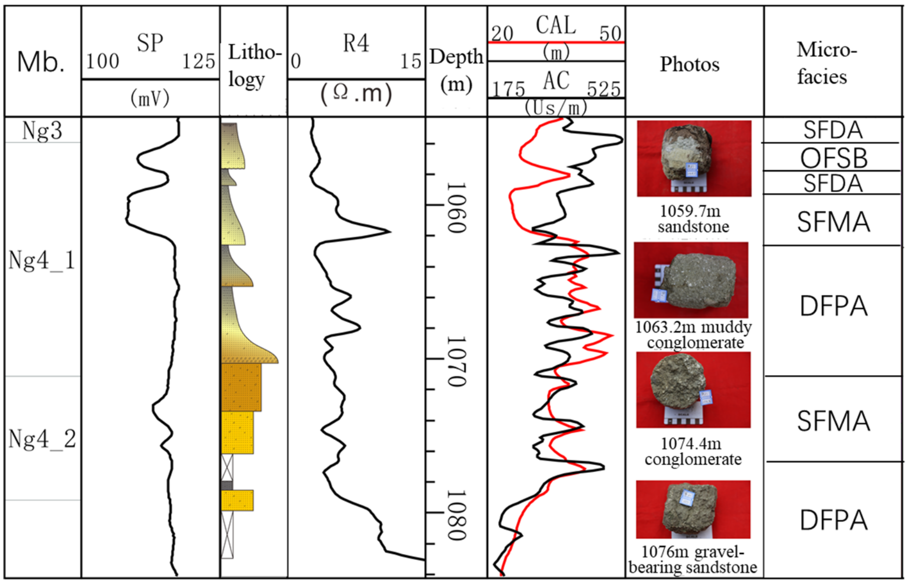

Figure 11. Sedimentary microfacies characteristics of well S87. DFPA: debris-flow in proximal alluvial fan, SFMA: stream flow in mid-alluvial fan, OFSB: overflow sand body, SFDA: sheet flow in distal alluvial fan.

Sheet flow in distal alluvial fan (SFDA) formed by unchanneled flow which is shallow and short lived and localized on the distal alluvial fan where channels become shallow and ill-defined. The thickness of SFDA is small, commonly less than 2 m. The lithology of SFDA is mainly mudstone and siltstone.

Braided channels outside alluvial fans (BCOA) BCOA develop outside the alluvial fan on the periphery of the Binxian uplift. The BCOA is mainly composed of medium sandstone and fine sandstone. The thickness of BCOA is commonly more than 2 m with an upward-fining rhythm.

There are significant differences in reservoir physical properties of different sedimentary microfacies (Figure 12). The porosity of SFMA ranges from 6.57% to 38.4%, with an average of 27.6%. The proportion of samples in SFMA with porosity higher than 30% account for 53.6 percent and samples with porosity between 20% and 30% account for 31.9 percent (Figure 12A). The BCOA has a porosity between 9% and 38.9%, with an average of 29%. Samples with porosity higher than 30% and samples with porosity between 20% and 30% both account for 44%. The porosity of OFSB, which ranges from 12.4% to 30.5% (average 22.8%), is lower than that of SFMA and BCOA. The porosity of OFSB mainly distributed in the range between 20% and 30%, accounts for 52.6%. The porosities of DFPA are from 20.5% to 23.8%, with an average of 22.6%. The SFDA is mainly mudstone, which is not a reservoir for petroleum. Thus, the SFMA and BCOA have relatively good reservoir quality. In contrast, the OFSB and DFPA have poor reservoir quality.

Different sedimentary microfacies were formed in different sedimentary environments and have different grain sizes, sorting, and particle arrangements, resulting in different primary porosities. The composition and texture of lithologies are controlled by the distribution of sedimentary microfacies. The SFMA and BCOA, which are formed by stable and continuous traction flow sedimentation in water bodies, have relatively high component maturity and good sorting, resulting in relatively high primary porosity. On the contrary, DFPA and OFSB were formed by rapid sedimentation of gravity flow, having poor sorting and mixed grains of different sizes with relatively low primary porosity and permeability. Therefore, microfacies have an important influence on primary porosity and permeability for alluvial glutenite reservoirs.

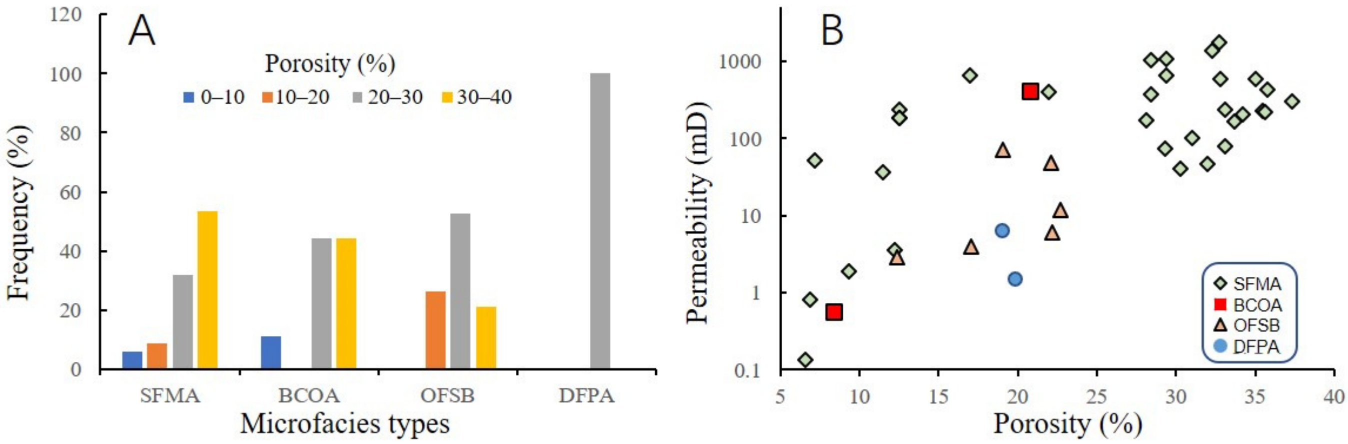

Figure 12. Differences in porosity and permeability of different microfacies. (**A**) Porosity differences in different microfacies types; (**B**) Cross plot of porosity and permeability of different microfacies. SFMA: stream flow in mid-alluvial fan, BCOA: braided channels outside alluvial fans. OFSB: overflow sand body, SFDA: sheet flow in distal alluvial fan.

5.1.3. Diagenesis Impact on Reservoir Properties

The porosities of SFMA have a wide range, from 6.57% to 38.4%, suggesting that besides sedimentary factors, there are other factors that affect the reservoir quality. Besides the depositional factors, reservoir quality is also controlled by diagenesis. Compaction is commonly an important factor affecting reservoir quality. The intensity of compaction is related to burial depth, grain composition, and rock texture [35–38]. The burial depth of the reservoir in the study area ranges from 900 m to 1200 m. The contact type of grains in the reservoir are mainly point contact or line contact. The main type of clay mineral in the study area is montmorillonite, the relative content of which is greater than 76%. These indicate that the diagenetic stage of the reservoir is mainly in the early diagenetic stage [39].

Lithofacies with high content of plastic components and poor sorting commonly have more intense compaction [40]. The SFMA and BCOA are mainly composed of feldspathic lithic quartz-sandstones and arkose, which have good pressure resistance. The lithologies in SFMA and BCOA commonly are well sorted. Thus, the compaction of SFMA and BCOA is relatively weak. DFPA is composed of gravel, sands, and muddy components, showing poor sorting. OFSB contains a large amount of muddy debris, which is plastic deformation components and can enhance mechanical compaction. Therefore, the compaction of DFPA and OFSB is stronger than that of SFMA and BCOA. The degree of pore reduction caused by compaction of DFPA and OFSB is higher than that of SFMA and BCOA.

The main cement in the study area is carbonate mineral. Carbonate cements in the reservoir range from 0 to 60.3%, with an average volume of 26%. The carbonate cements occur mainly as pore-filling cements, which could occupy intergranular pores. The plot of volume of carbonate cement and porosity show that there is an inverse relationship between calcite content and porosity (Figure 13A). Thus, the volume of calcite cements is another important factor influencing the alluvial glutenite reservoir quality. High calcite cement content commonly results in low porosity and permeability.

The distribution of calcite cementation is not uniform in the reservoir. Analysis of cores show that intense calcite cementation commonly develops at the base of SFMA and BCOA and near the sandstone–mudrock contacts. This indicates that the source of calcium carbonate for calcite cement in the reservoir mainly came from around the mudstone. Some diagenetic evolution processes in mudstone, such as conversion of smectite to illite, illitization of kaolinite, dissolution of K-feldspar, and maturation of kerogen, can provide the necessary ions for carbonate cement formation [16,41–44]. Dissolution of carbonate from mudstone can diffuse into sandstone, which might further promote carbonate cementation near sandstone–mudrock contacts [39,45].

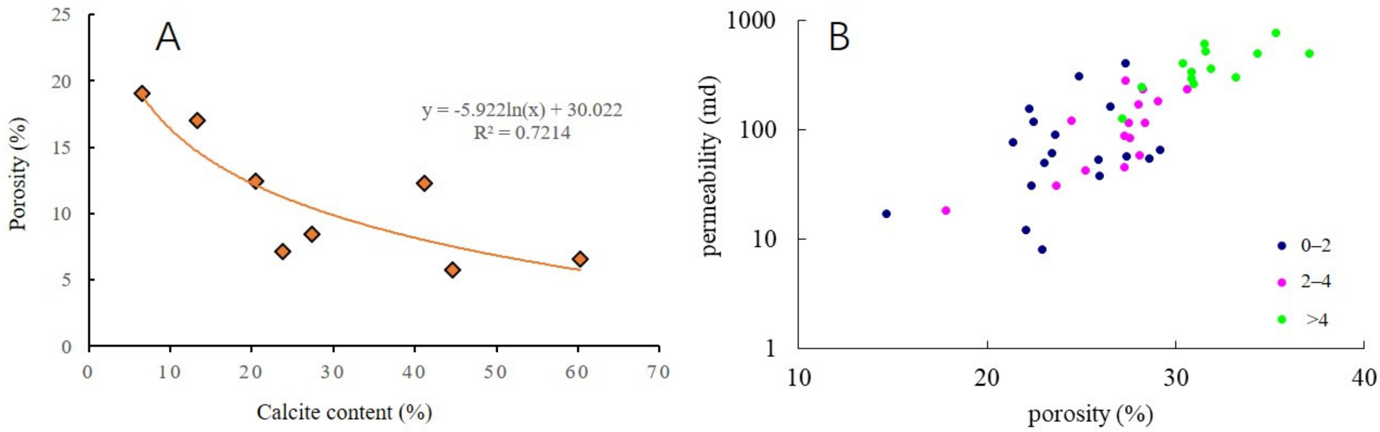

Figure 13. Influence of calcite content and single sand body thickness on reservoir quality. (**A**) Plot of calcite content versus porosity; (**B**) Plot of porosity and permeability of different single sand body thickness.

Because there is carbonate cement in the reservoir sourced from adjacent mudstone, thin sandstones are commonly cemented pervasively, while thick single sandstones are cemented at the base and top part, leaving the middle part with less cement. The plot of porosity versus permeability of different thicknesses of individual sandstones show that sandstones with large thicknesses also have high porosity and permeability (Figure 13B). Reservoirs with thicknesses more than 4m commonly have high porosity (>30%) and high permeability (>200 mD). The porosity and permeability of reservoirs with thicknesses between 2 m and 4 m mainly range from 24% to 30% and from 20 mD to 200 mD, respectively. The reservoir with a thickness less than 2m commonly has low porosity and permeability, mainly less than 26% and 100 mD, respectively. Therefore, individual glutenite thickness is also an important influencing factor on reservoir quality.

Unstable components are prone to be dissolved during diagenetic processes. In the study area, dissolution of feldspar, rock fragments, and carbonate cement are commonly observed, and secondary dissolution pores form during this process (Figure 7A–E). These indicate that dissolution occurred in the reservoir, forming secondary dissolution pores, which have been proved to commonly improve reservoir quality [16,21]. Authigenic kaolinites were found to be one of the important clay minerals in the study area, with an average relative content of 17%. Kaolinite commonly formed by dissolution of feldspar under acidic conditions and the formation of kaolinite is commonly due to dissolution of feldspars by meteoric waters during early diagenesis under a shallow burial depth [46,47]. The development of kaolinite suggests that incursion of meteoric waters occurred in the early stage of diagenesis, causing dissolution of feldspar [46,47]. Because the burial depth of the reservoir is shallower than 1200 m in the study area, the organic matter in the Guantao formation is unmatured, suggesting large amounts of organic acids were not being released during diagenesis process [20,48]. Thus, the dissolution fluid for the formation of secondary pores in the study area is mainly meteoric waters instead of organic acid.

5.2. Control of Reservoir Properties on Hydrocarbon Accumulation

Oil-bearing properties in the alluvial glutenite reservoir are strongly heterogeneous. According to the liquid production situation, reservoirs can be divided into oil layers, oil-water layers, water layers, and dry layers. The porosity and permeability of oil layers, oil-water layers, water layers, and dry layers were put into one cross plot system (Figure 14A). It is shown that oil layers have the highest porosity and permeability, followed by oil-water layers and water layers. The dry layers have the lowest porosity and permeability. The porosity and permeability at the boundary between oil-bearing layers and non-oil bearing layers is the lower limit of the physical properties of effective reservoirs. According to the cross plot, the lower limit of the physical properties of effective reservoirs is a porosity of 27% and permeability of 225 mD (Figure 14A).

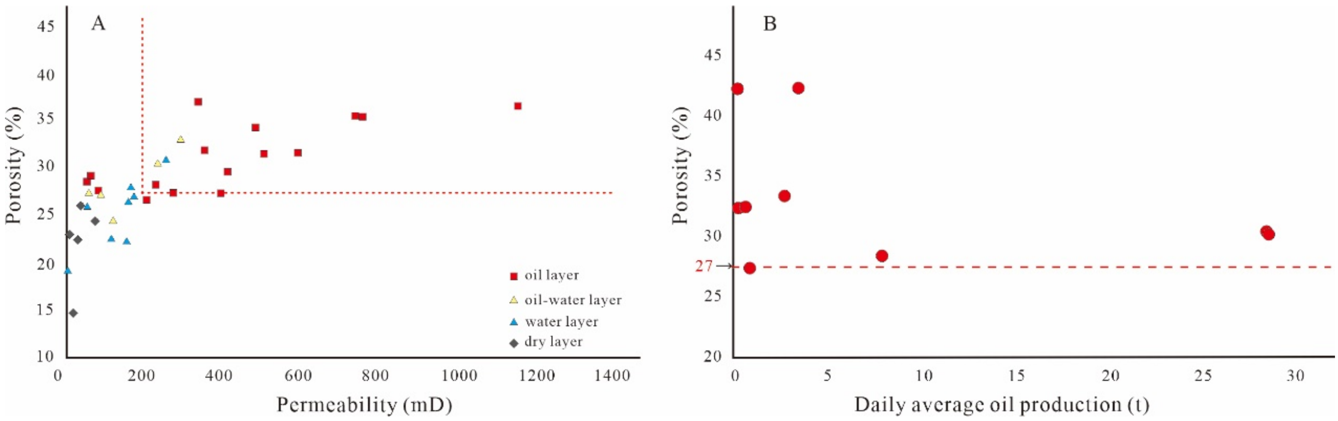

Figure 14. Control of reservoir properties on hydrocarbon accumulation. (**A**) Cross plot of porosity versus permeability of different oil-bearing layers. (**B**) Cross between average porosity and daily average oil production.

The analysis of the relationship between the daily average oil production and porosity shows that only the reservoirs with porosities greater than 27% have oil production capacity, indicating that the reservoir porosity has an important influence on petroleum saturation and verifying the accuracy of the lower limit of the porosity at 27% (Figure 14B). Therefore, this reservoir property has an important influence on hydrocarbon accumulation. Reservoirs with porosity lower than 27% and/or permeability lower than 225 mD cannot accumulation oil in the study area.

6. Conclusions

(1) Pore types in the study area mainly include residual intergranular pores, intergranular dissolved pores, intragranular dissolved pores, and mold pores. The residual intergranular pores and intergranular dissolved pores are the main pore types. Most samples have porosity greater than 15% and permeability is mainly concentrated between 50 mD and 500 mD. The lithology type, microfacies, and diagenesis have significant impacts on the reservoir quality.

(2) The reservoir qualities of very fine sandstone and fine sandstone are better than those of conglomerate and gravel-bearing sandstone. Sorting is one of the important factors affecting alluvial glutenite reservoir quality. Oil-bearing samples commonly have sorting coefficients less than 2 while non-oil-bearing samples have sorting coefficients larger than 2. There are significant differences in reservoir physical properties of different sedimentary microfacies. The stream flow in mid-alluvial fan (SFMA) and braided channels outside alluvial fans (BCOA) have relatively weak compaction and good reservoir quality. On the contrast, the overflow sand body (OFSB) and debris-flow in proximal alluvial fan (DFPA) have relatively strong compaction and poor reservoir quality.

(3) Calcite is the main cement in the study area. Calcite cementation commonly developed at the base of SFMA and BCOA and near the sandstone–mudrock contacts. The source of calcium carbonate for calcite cement mainly came from surrounding mudstone. High calcite cement content commonly results in low porosity and permeability. Individual glutenite thickness is also an important influencing factor on reservoir quality. Reservoirs with large thicknesses (>4 m) have high porosity and permeability. Dissolution occurred in the reservoir, forming secondary dissolution pores and improving reservoir quality. The dissolution fluid for formation of secondary pores is mainly meteoric waters instead of organic acid.

(4) The reservoir properties have important influence on hydrocarbon accumulation. The lower limit of physical properties of effective reservoirs is a porosity of 27% and permeability of 225 mD. Reservoirs with porosities lower than the limit of physical properties cannot accumulate oil.

Author Contributions: Conceptualization, Q.L.; methodology, X.Y.; software, Y.Z. and Y.H.; formal analysis R.T. and J.L.; investigation, Q.L.; writing—original draft preparation, Q.L.; review X.Y.; funding acquisition, Q.L. and X.Y. All authors have read and agreed to the published version of the manuscript.

Funding: This study was financially supported by the National Natural Science Foundation of China (Grant No. 42372146 and 41972107). The Strategic Cooperation Technology Projects of CNPC and CUPB (ZLZX 2020-02).

Data Availability Statement: Data are contained within the article.

Acknowledgments: We are grateful to the Exploration and Development Research Institute of Shengli Oilfield for providing samples and data access, and for permission to publish the results.

Conflicts of Interest: The authors declare no conflicts of interest.

References

1. Jiang, Z. *Sedimentology*; Petroleum Industry Press: Beijing, China, 2003; pp. 60–123. (In Chinese)
2. Rogers, J.P. New reservoir model from an old oil field: Garfield conglomerate pool, Pawnee County, Kansas. *AAPG Bull.* **2007**, *91*, 1349–1365. [CrossRef]
3. Mahmic, O.; Dypvik, H.; Hammer, E. Diagenetic influence on reservoir quality evolution, examples from Triassic conglomerates/arenites in the Edvard Grieg field, Norwegian North Sea. *Mar. Petrol. Geol.* **2018**, *93*, 247–271. [CrossRef]
4. Kang, X.; Hu, W.; Cao, J.; Wu, H.; Xiang, B.; Wang, J. Controls on reservoir quality in fan-deltaic conglomerates: Insight from the Lower Triassic Baikouquan Formation, Junggar Basin, China. *Mar. Pet. Geol.* **2019**, *103*, 55–75. [CrossRef]
5. Zhang, K.; Wu, S.; Zhong, Y.; Shi, L. Modal distribution of pore-throat size in sandy conglomerates from an alluvial fan environment: Lower Karamay Formation, Junggar Basin, West China. *Mar. Pet. Geol.* **2020**, *117*, 104391. [CrossRef]
6. Schmidt, G.A.; Pemberton, S.G. Stratigraphy and paleogeography of a conglomeratic shoreline: The notikewin member of the Spirit River Formation in the Wapiti area of west–central Alberta. *Bull. Can. Petrol. Geol.* **2004**, *52*, 57–76. [CrossRef]
7. Jia, H.; Ji, H.; Li, X.; Zhou, H.; Wang, L.; Gao, Y. A retreating fan–delta system in the Northwestern Junggar Basin, northwestern China—Characteristics, evolution and controlling factors. *J. Asian Earth Sci.* **2016**, *123*, 162–177. [CrossRef]
8. Wei, W.; Zhu, X.M.; Tan, M.X.; Wu, C.B.J.; Guo, D.B.; Su, H.; Jiang, F.H. Facies controls on the distribution of diagenetic alterations in fan delta deposits: A case study from the Lower Cretaceous sandstone, Chagan Sag, Inner Mongolia, China. *Geol. J.* **2017**, *52*, 539–558. [CrossRef]
9. Wang, Y.; Dong, C.; Lin, C.; Hou, Q. The Main Controlling Factors of Glutenite Development and Their Impacts on Oil Energy Extraction. *Energies* **2021**, *14*, 1807. [CrossRef]
10. Zhang, S.C.; Zou, N.N.; Shi, J.A.; Chang, Q.S.; Lu, X.C.; Chen, B. Depositional model of the triassic Baikouquan Formation in Mabei area of Junggar Basin. *Oil Gas Geol.* **2015**, *36*, 640–649, (In Chinese with English Abstract).
11. Hart, B.S.; Plint, A.G. Stratigraphy and sedimentology of shoreface and fluvial conglomerates: Insights from the Cardium Formation in NW Alberta and adjacent British Columbia. *Bull. Can. Petrol. Geol.* **2003**, *51*, 437–464. [CrossRef]
12. Morad, S.; Al–Ramadan, K.; Ketzer, J.M.; De Ros, L.F. The impact of diagenesis onthe heterogeneity of sandstone reservoirs: A review of the role of depositional facies and sequence stratigraphy. *AAPG Bull.* **2010**, *94*, 1267–1309. [CrossRef]
13. Yuan, G.; Cao, Y.; Qiu, L.; Chen, Z. Genetic mechanism of high-quality reservoirs in Permian tight fan delta conglomerates at the northwestern margin of the Junggar Basin, northwestern China. *AAPG Bull.* **2017**, *101*, 1995–2019. [CrossRef]
14. Cant, D.J.; Ethier, V.G. Lithology–dependent diagenetic control of reservoir properties of conglomerates, Falher Member, Elmworth Field, Alberta. *AAPG Bull.* **1984**, *68*, 1044–1054.
15. Ma, B.; Cao, Y.; Eriksson, K.A.; Jia, Y.; Gill, B.C. Depositional and diagenetic controls on deeply-buried Eocene sublacustrine fan reservoirs in the Dongying Depression, Bohai Bay Basin, China. *Mar. Pet. Geol.* **2017**, *82*, 297–317. [CrossRef]
16. Bello, A.M.; Butt, M.N.; Hussain, A.; Amao, A.O.; Olariu, C.; Koeshidayatullah, A.I.; Malik, M.H.; Al-Hashem, M.; Al-Ramadan, K. Impact of depositional and diagenetic controls on reservoir quality of syn-rift sedimentary systems: An example from Oligocene-Miocene Al Wajh Formation, northwest Saudi Arabia. *Sediment. Geol.* **2023**, *446*, 106342. [CrossRef]
17. Jamil, M.; Siddiqui, N.A.; Rahman, A.H.B.A.; Ibrahim, N.A.; Ismail, M.S.B.; Ahmed, N.; Usman, M.; Gul, Z.; Imran, Q.S. Facies Heterogeneity and Lobe Facies Multiscale Analysis of Deep-Marine Sand-Shale Complexity in the West Crocker Formation of Sabah Basin, NW Borneo. *Appl. Sci.* **2021**, *11*, 5513. [CrossRef]

18. Jamil, M.; Siddiqui, N.A.; Ahmed, N.; Usman, M.; Umar, M.; Rahim, H.; Imran, Q.S. Facies Analysis and Sedimentary Architecture of Hybrid Event Beds in Submarine Lobes: Insights from the Crocker Fan, NW Borneo, Malaysia. *J. Mar. Sci. Eng.* **2021**, *9*, 1133. [CrossRef]
19. Li, Q.; Jiang, Z.; Liu, K.; Zhang, C.; You, X. Factors controlling reservoir properties and hydrocarbon accumulation of lacustrine deep-water turbidites in the Huimin Depression, Bohai Bay Basin, East China. *Mar. Pet. Geol.* **2014**, *57*, 327–344. [CrossRef]
20. Mansurbeg, H.; Morad, S.; Salem, A.; Marfil, R.; El-Ghali, M.A.K.; Nystuen, J.P.; Caja, M.A.; Amorosi, A.; Garcia, D.; La Iglesia, A. Diagenesis and reservoir quality evolution of palaeocene deep-water, marine sandstones, the Shetland-Faroes Basin, British continental shelf. *Mar. Pet. Geol.* **2008**, *25*, 514–543. [CrossRef]
21. Bello, A.M.; Al-Ramadan, K.; Babalola, L.O.; Alqubalee, A.; Amao, A.O. Impact of grain-coating illite in preventing quartz cementation: Example from permo-carboniferous sandstone, Central Saudi Arabia. *Mar. Pet. Geol.* **2023**, *149*, 106073. [CrossRef]
22. Anovitz, L.M.; Cole, D.R. Characterization and analysis of porosity and pore structures. *Rev. Mineral. Geochem.* **2015**, *80*, 61–164. [CrossRef]
23. Bultreys, T.; Van Hoorebeke, L.; Cnudde, V. Multi-scale, micro-computed tomography-based pore network models to simulate drainage in heterogeneous rocks. *Adv. Water Resour.* **2015**, *78*, 36–49. [CrossRef]
24. Yu, F.; Koyi, H. Cenozoic tectonic model of the Bohai Bay Basin in China. *Geol. Mag.* **2016**, *153*, 866–886. [CrossRef]
25. Guo, J.X.; Guo, W.P.; Liu, B.N.; Cao, Z. Sedimentary Microfacies Types and Space Distribution of the Third Member of Guantao Formation in Dalujia Area of Huimin Sag. *J. Earth Sci. Environ.* **2015**, *37*, 66–75. (In Chinese)
26. Tian, M.R. Stratigraphic sequence framework of Neogene Guantao formation, Dongying sag. *Pet. Geol. Recovery Effic.* **2010**, *17*, 1–3+8. (In Chinese)
27. Wu, Y.L.; Fan, T.L.; Zhang, S.P.; Dai, Q.D.; Guo, J.X.; Li, H. Upper Tertiary Sequence Stratigraphy and Sedimentary System in Jiyang Depression. *J. Oil Gas Technol.* **2005**, *27*, 15–17+5. (In Chinese)
28. Li, Y.; Li, S.Y.; Yue, S.C.; Wang, Z.C.; Li, Z.; Wu, C.D.; Li, X. Sedimentary Architectural elements of upper member of the Guantao Formation in Guantao area, Shengli Oilfield. *Sci. Geol. Sin.* **2002**, *37*, 219–230+260. (In Chinese)
29. Xie, Q.H.; Dai, J.S.; Ma, X.M. Control of Faults of Guantao Formation on Hydrocarbon Accumulation in Jiyang Depression. *Xinjiang Pet. Geol.* **2007**, *28*, 486–489. (In Chinese)
30. Huang, J.Z. Hydrocarbon reservoir models on the slope zone of salient: Taking Shanjiasi oil field of Binxian salient in the Dongying depression as an example. *J. Stratigr.* **2007**, *31* (Suppl. 2), 593–598. (In Chinese)
31. Folk, R.L. *Petrology of Sedimentary Rocks*; Hemphill Publishing: Austin, TX, USA, 1980; p. 182.
32. Cade, C.A.; Evans, I.J.; Bryant, S.L. Analysis of permeability controls e a new approach. *Clay Miner.* **1994**, *29*, 491–501. [CrossRef]
33. Schmid, S.; Worden, R.H.; Fisher, Q.J. Diagenesis and reservoir quality of the Sherwood Sandstone (Triassic), Corrib field, Slyne Basin, west of Ireland. *Mar. Pet. Geol.* **2004**, *21*, 299–315. [CrossRef]
34. Sun, S.; Shu, L.; Zeng, Y.; Cao, J.; Feng, Z. Porosity-permeability and textural heterogeneity of reservoir sandstones from the lower Cretaceous Putaohua member of Yaojia Formation, Weixing oilfield, Songliao Basin, Northeast China. *Mar. Pet. Geol.* **2007**, *24*, 109–127. [CrossRef]
35. Lima, R.D.; De Ros, L.F. The role of depositional setting and diagenesis on the reservoir quality of Devonian sandstones from the Solimoes Basin, Brazilian Amazonia. *Mar. Pet. Geol.* **2002**, *19*, 1047–1071. [CrossRef]
36. Gier, S.; Worden, R.H.; Johns, W.D.; Kurzweil, H. Diagenesis and reservoir quality of Mioceme sandstones in the Vienna Basin, Austria. *Mar. Pet. Geol.* **2008**, *25*, 681–695. [CrossRef]
37. Pittman, E.D.; Larese, R.E. Compaction of lithic sands: Experimental results and applications. *AAPG Bull.* **1991**, *75*, 1279–1299.
38. Chen, D.; Pang, X.; Jiang, Z.; Zeng, J.; Qiu, N.; Li, M. Reservoir characteristics and their effects on hydrocarbon accumulation in lacustrine turbidites in the Jiyang super-depression, Bohai Bay Basin, China. *Mar. Pet. Geol.* **2009**, *26*, 149–162. [CrossRef]
39. Foscolos, A.E.; Powell, T.G.; Gunther, P.R. The use of clay minerals and inorganic and organic geochemical indicators for evaluating the degree of diagenesis and oil generating potential of shales. *Geochim. Cosmochim Acta* **1976**, *40*, 953–966. [CrossRef]
40. Gluyas, J.; Cade, C.A. Prediction of porosity in compacted sands. In *Reservoir Quality Prediction in Sandstones and Carbonates*; AAPG Memoir: Tulsa, OK, USA, 1997; Volume 69, pp. 19–28.
41. Bello, A.M.; Jones, S.J.; Gluyas, J.; Al-Ramadan, K. Impact of Grain-Coating Clays on Porosity Preservation in Paleocene Turbidite Channel Sandstones: Nelson Oil Field, UK Central North Sea. *Minerals* **2022**, *12*, 555. [CrossRef]
42. El-Ghali, M.A.K.; Shelukhina, O.; Abbasi, I.A. Depositional and sequence stratigraphic controls on diagenesis in the Upper Cambrian-Lower Ordovician Barik Formation, central Oman: Implications for prediction of reservoir porosity in a hybrid-energy delta system. *Mar. Pet. Geol.* **2024**, *160*, 106611. [CrossRef]
43. Carvalho, M.V.F.; De Ros, L.F.; Gomes, N.S. Carbonate cementation patterns and diagenetic reservoir facies in the Campos Basin Cretaceous turbidites, offshore eastern Brazil. *Mar. Pet. Geol.* **1995**, *12*, 741–758. [CrossRef]
44. Dutton, S.P. Calcite cement in Permian deep-water sandstones, Delaware Basin, west Texas: Origin, distribution, and effect on reservoir properties. *AAPG Bull.* **2008**, *92*, 765–787. [CrossRef]
45. Milliken, K.L.; Land, L.S. The origin and fate of silt sized carbonate in subsurface Miocenee Oligocene mudstones, south Texas Gulf Coast. *Sedimentology* **1993**, *40*, 107–124. [CrossRef]
46. Mansurbeg, H.; El-Ghali, M.A.K.; Morad, S.; Plink-Bjorklund, P. The impact of meteoric water on the diagenetic alterations in deep-water, marine siliciclastic turbidites. *J. Geochem. Explor.* **2006**, *89*, 254–258. [CrossRef]

47. Mansurbeg, H.; De Ros, L.F.; Morad, S.; Ketzer, J.M.; El-Ghali, M.A.K.; Caja, M.A.; Othman, R. Meteoric-water diagenesis in late Cretaceous canyou-fill turbidite reservoirs from the Espirito Santo Basin, eastern Brazil. *Mar. Pet. Geol.* **2012**, *37*, 7–26. [CrossRef]
48. Morad, S.; Ketzer, J.M.; De Ros, L.F. Spatial and temporal distribution of diagenetic alterations in siliciclastic rocks: Implications for mass transfer in sedimentary basins. *Sedimentology* **2000**, *47*, 95–120. [CrossRef]